STUDY OF THE NEUTRON LAUE DIFFRACTION IN LARGE SILICON CRYSTAL FOR THE BRAGG ANGLES CLOSE TO $\pi/2$

E. O. Vezhlev, V. V. Voronin, I. A. Kuznetsov, S. Yu. Semenikhin, V. V. Fedorov
Petersburg Nuclear Physics Institute, Gatchina, Russia

Abstract

The Laue diffraction on (220) plane of large (~ 200 mm) silicon crystal was investigated for the Bragg angles close to $\pi/2$. It was demonstrated that the effective neutron absorption length for the low-absorbed Bloch wave can reach about 3 m instead of 40 cm for the non-diffracted neutrons. Therefore, we saw reasonable reflected neutron beam intensity for the Bragg angles about 88^0 and it was possible to observe specific dynamical diffraction effects for Laue neutron diffraction with such Bragg angles in the extremely thick crystal. Experimental results are in good agreement with theoretical predictions for both one-crystal scheme and for two-crystal scheme of setup.

Introduction

The crystal-diffraction experiment to test weak equivalence principle for the neutron was recently proposed [1, 2]. It is based on the essential magnification of external affect on the neutron diffracting under Laue for the Bragg angles close to the right one. Recently we observed an additional enhancement factor of small effects exerting influence on a neutron undergoing Laue diffraction at such Bragg angles [3]. This factor arises due to the time of diffracted neutron delay inside the crystal and is proportional to $tan^2(\theta_B)$. Its value can reach 10^3. In the aggregate with diffraction enhancement factor, which is also known as decreasing of diffracting neutron effective mass [4], the total diffraction enhancement factor may be as large as 10^9. So, it becomes interesting to try to utilize this enhancment phenomenon for investigation of external affects acting on a diffracting neutron.

In the experiment we were working with two-crystal scheme of Laue diffraction in large $\oslash 150 \times 220$ mm^3 silicon crystal. The working crystalographic plane is (220). Experimental setup is based on direct neutron beam collimation with system of slits which allows us to observe neutron beam shift on the exit surface of the crystal. In this consideration specific dynamical diffraction effects become very significant. First of all, effect of anomalous transmission or Borrmann effect [5] should be taken into account. This effect gives different absorption lengths for different types of Bloch waves excited in crystal (in fact for low-absorbed wave absorption length is by one order of magnitude higher than for non-diffracted neutrons). Borrmann effect was investigated for x-rays more than fifty years ago and its detailed description can be found in [5]. Theoretical consideration of this effect for neutrons can be found in [6] and also in [7, 8].

1. Neutron Laue diffraction in perfect crystals

Here we consider the symmetrical Laue diffraction scheme in a transparent crystal with the system of crystallographic planes described by the reciprocal lattice vector g normal to the planes (see Fig. 1), $g = 2\pi/d$, d is the interplanar distance. In this case, the neutron wave function in a crystal will be a superposition of Bloch waves

$$\psi^j(\mathbf{r}) = a_j(\mathbf{r})\, e^{(i\mathbf{k}_j\mathbf{r})}. \qquad (1)$$

In two-beam approximation (1) becomes a superposition of two Bloch waves $\psi^{(1)}$ and $\psi^{(2)}$ corresponding to two branches of the dispersion surface [6]

$$\psi^{1,2} = \psi_0^{1,2} + \psi_{\mathbf{g}}^{1,2}, \tag{2}$$

where ψ_0 – is the wave function of direct beam and $\psi_{\mathbf{g}}$ – is the wave function of reflected beam. In the plane wave approximation neutron currents directions (Fig. 1) in crystal can be defined for each Bloch wave field separately and, neglecting the fast oscillating interference terms, are given by

$$\mathbf{j}_{1,2} = \frac{\hbar|\mathbf{k}|}{m}\left(\mathbf{n}_0\left|\psi_0^{1,2}\right|^2 + \mathbf{n}_g\left|\psi_{\mathbf{g}}^{1,2}\right|^2\right), \tag{3}$$

where $\mathbf{n}_0$ and $\mathbf{n}_{\mathbf{g}}$ – are the unit wave vectors corresponded to direct and reflected directions.

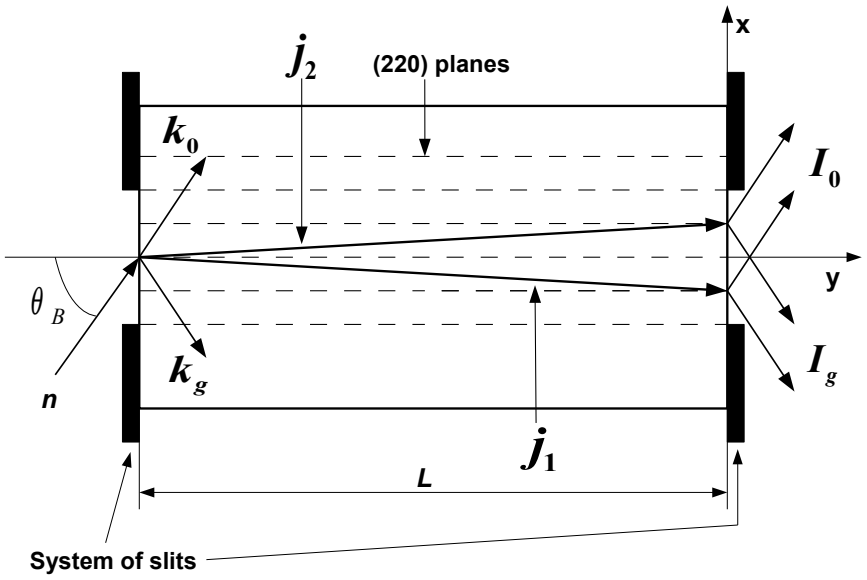

Figure 1: Laue diffraction in single crystal. $\mathbf{j}_1$ and $\mathbf{j}_2$ – directions of neutron currents.

Neutron currents in crystal are bounded by the size of so-called "Borrmann fan". It's convenient to describe distribution of "Borrmann fan" by using the parameter of deviation from exact Bragg condition

$$\Gamma = \frac{tg\,(\theta)}{tg\,(\theta_B)} = \frac{x}{2Ltg\,(\theta_B)}. \tag{4}$$

Under this term "Borrmann fan" lies between $-1 < \Gamma < 1$. One can also describe the wave amplitudes inside the crystals by the terms of Γ. They are given by the following expressions:

$$a_0^{1,2}\,(\Gamma) = \frac{1-\Gamma}{2\,(1+\Gamma)\sqrt{1-\Gamma^2}}, \tag{5}$$

$$a_{\mathbf{g}}^{1,2}\,(\Gamma) = \frac{1}{2\sqrt{1-\Gamma^2}}. \tag{6}$$

Finally without taking interference effects into account one obtains the intensity profile on the exit surface of crystal [6]

$$R_{0,\mathbf{g}}(\Gamma) = [(a_0^{1,2}(\Gamma))^2 + (a_{\mathbf{g}}^{1,2}(\Gamma))^2]\frac{1}{(1-\Gamma^2)\sqrt{1-\Gamma^2}}. \tag{7}$$

The intensity profile (7) shows increase of the intensity on the margins of the "Borrmann fan" (when $|\Gamma| \to 1$). This effect in neutron diffraction was first observed in [9] and explained in [10].

2. Influence of absorption

For the case of non zero absorption the amplitudes of diffracted in Bragg direction waves are given by [6]:

$$\begin{array}{l} a_{\mathbf{g}}^{1,2}(\Gamma) = \frac{e^{-\Sigma_0 L_{eff}}}{\sqrt{2}(1-\Gamma^2)^{1/4}} \times \\ \times \left(\sin^2\left(\frac{A}{\sqrt{1-\Gamma^2}}\right) + \sinh^2\left(\Sigma_{\mathbf{g}} L_{eff}\sqrt{1-\Gamma^2}\right)\right)^{1/2}, \end{array} \tag{8}$$

where $\Sigma_0 = \frac{1}{V}\sum\limits_i \sigma_i^I$ and $\Sigma_{\mathbf{g}} = \frac{1}{V}\sum\limits_i \exp(-i\mathbf{g}\mathbf{r_i})\sigma_i^I$ – zero and g-harmonic of absorption (σ_i^I – is total cross-section of absorption and incoherent scattering); $L_{eff} = L/\cos\theta_B$ – effective crystal length; $A = (\pi L)/\xi_{\mathbf{g}}$, where $\xi_{\mathbf{g}}$ – is so called extinction length which describes the period of "Pendellosung" oscillations [6].

With increasing of crystal length and consequently the $(\pi L)/\xi_{\mathbf{g}}$ value one can average the amplitudes over "Pendellosung" oscillation period. Therefore (8) can be simplified:

$$a_{\mathbf{g}}^{1,2}(\Gamma) = \frac{e^{-\Sigma_0 L_{eff}}}{2(1-\Gamma^2)^{1/4}}\left(\pm\cosh 2\left(\Sigma_{\mathbf{g}} L_{eff}\sqrt{1-\Gamma^2}\right)\right). \tag{9}$$

In case of diffraction in thick crystal when $\Sigma_{\mathbf{g}} L_{eff} >> 1$ what gives us $\exp(-\Sigma_{\mathbf{g}} L_{eff}) << 1$, the amplitudes (9) become:

$$a_{\mathbf{g}}^{1,2}(\Gamma) = \frac{\exp\left(-L_{eff}\left(\Sigma_0 \pm \Sigma_{\vec{g}}\sqrt{1-\Gamma^2}\right)\right)}{4(1-\Gamma^2)^{1/4}}. \tag{10}$$

The amplitudes value for transmitted wave can be obtained similar to (10)

$$a_0^{1,2}(\Gamma) = \frac{\exp\left(-L_{eff}\left(\Sigma_0 \pm \Sigma_{\mathbf{g}}\sqrt{1-\Gamma^2}\right)\right)}{4(1-\Gamma^2)^{1/4}}\sqrt{\frac{1-\Gamma}{1+\Gamma}}. \tag{11}$$

The intensity profile at the exit surface of the crystal after averaging over interference term will be:

$$\begin{array}{l} R_0 = (a_0^1)^2 + (a_0^2)^2, \\ R_{\mathbf{g}} = \left(a_{\mathbf{g}}^1\right)^2 + \left(a_{\mathbf{g}}^2\right)^2. \end{array} \tag{12}$$

From equations (10, 11) one can see that for the second type of two Bloch waves ($\psi_{0,\mathbf{g}}^1, \psi_{0,\mathbf{g}}^2$) absorption will be much more weaker than for the first one. In fact this is the direct consequence of anomalous transmission or Borrmann effect. This effect gives an opportunity for the diffracting neutrons to pass through extremely large (we worked with 220 mm of silicon) crystals without considerable losses of intensity.

3. Experimental observation of Borrmann effect

Experimental studies were done at WWR-M research reactor (PNPI, Gatchina). Neutron Laue diffraction with Bragg angles close to $\pi/2$ was investigated both for one-crystal (Fig. 1) and for two-crystal (Fig. 2) schemes on (220) crystallographic planes of large ($\oslash 150 \times 220$ mm^3) silicon crystal with interplanar distance $d = 1,92{\cdot}10^{-8}$ cm. Silicon crystal was mounted in thermostat for minimization of thermal deformation effect in crystalline medium. The necessary high collimation of the neutron beam was provided by the first crystal with slits placed on entrance and exit faces.

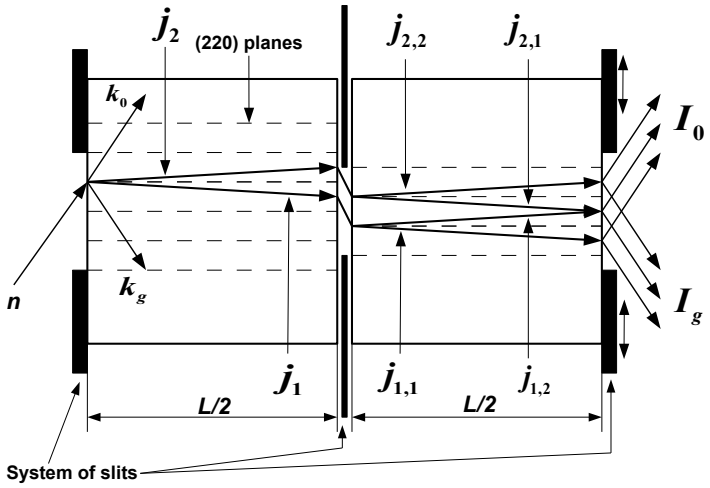

Figure 2: Two-crystal scheme of Laue diffraction. Collimating slits are mounted at the entrance and exit surfaces of the crystal. $\mathbf{j}_1$ and $\mathbf{j}_2$ – directions of neutron currents in the first crystal; $\mathbf{j}_{i,j}$ $(i,j = 1,2)$ – directions of neutron currents in the second crystal.

In the experiment we took the intensity dependences for one- and two-crystal schemes of Laue diffraction on a Bragg angle value (Fig. 3). Bragg angle value reached 88^0. On the Fig. 3 one can also see effective crystal length value $L_{eff} = L/\cos\theta_B$ that reaches 6 meteres for 88^0. Theoretical calculations were made for silicon absorption length $L_{abs} = 40$ cm. The g-harmonic of the linear absorption coefficient can be presented by the following formula

$$\Sigma_{\mathbf{g}} = \Sigma_0 \left(1 - \delta_{\mathbf{g}}\right) \tag{13}$$

where $\delta_{\mathbf{g}}$ – is a free parameter. The best agreement with experiment had been obtained for $\delta_{\mathbf{g}} = 0,012$. In this case the linear absorption coefficient value for the first Bloch wave type is

$$\Sigma_1 = \Sigma_0(2 - \delta_{\mathbf{g}}) = 0,05 \text{ cm}^{-1},$$

and for the second Bloch wave type is

$$\Sigma_2 = \Sigma_0\delta_{\mathbf{g}} = 0,003 \text{ cm}^{-1}.$$

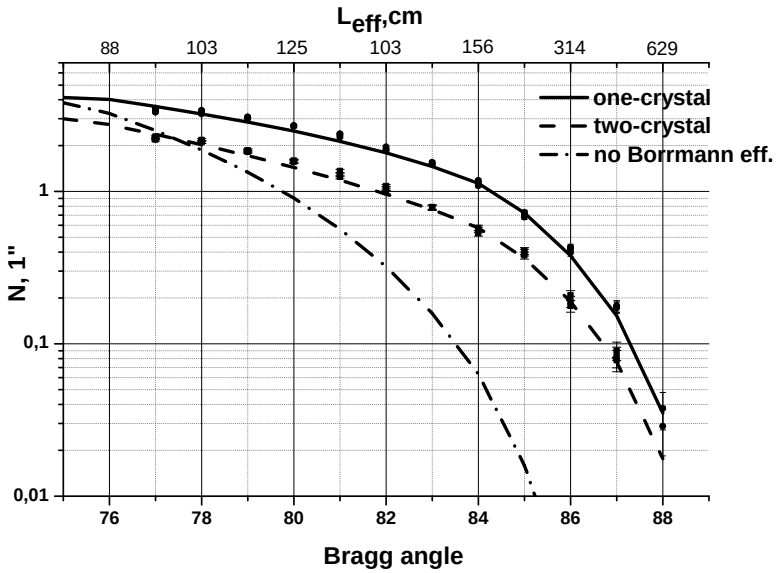

Figure 3: Intensity dependence on a Bragg angle value for one- and two-crystal schemes of the setup for silicon crystal. Crystallographic plane (220). Crystal thickness $L = 220$ mm. Dots stand for the experimental data and lines for theoretical predictions.

For the two-crystal scheme of Laue diffraction the intensity profile for tramsmitted beam (Fig. 2) can be derived from

$$\begin{aligned} R_0 &= \tfrac{1}{2} R_0\left(L/2\right) R_0\left(L/2\right) = ... \\ ... &= \tfrac{1}{2}\left[\left(a_0^1\left(L/2\right)\right)^2 + \left(a_0^2\left(L/2\right)\right)^2\right]^2 . \end{aligned} \tag{14}$$

Dependence of intensities values ratio on a Bragg angle for one- and two-crystal schemes is shown on the Fig. 4. Taking diffraction focusing [11] and Borrmann effects into account theory predicts increasing of intensity for the two-crystal scheme in comparison with one-crystal scheme when diffraction is going with normal Bragg angles. But when Bragg angles are tending to $\pi/2$ the intensity in two-crystal scheme becomes lower than for one-crystal scheme. This fact coincides with our experimental setup geometry and also corroborates results of plane wave approximation for Laue diffraction case.

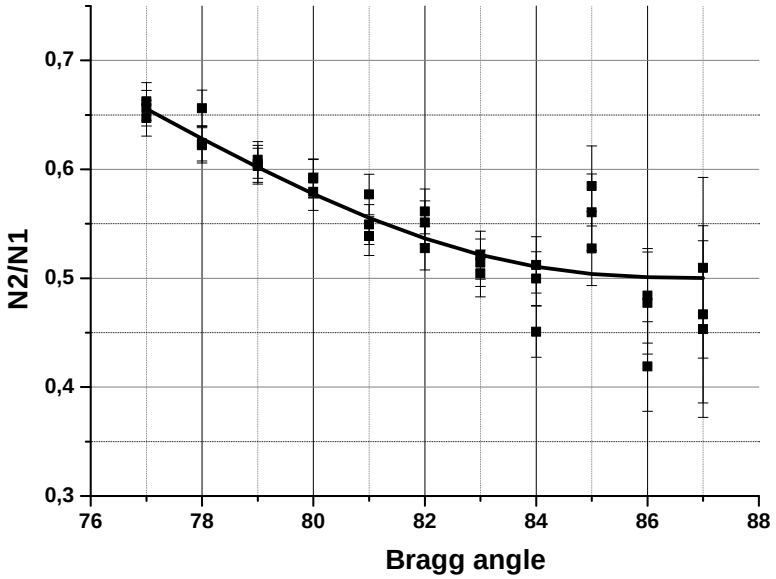

Figure 4: Dependence of intensities values ratio on a Bragg angle for one- and two-crystal schemes of the setup for silicon crystal. Solid line is a theoretical curve.

4. Influence of an external force on a Laue diffracting neutron

For the neutron Laue diffraction in deformed crystals special theory was developed [10]. In this theory effective "Kato force" f_k is imposed. This force describes diffracting neutron propagation inside weakly deformed crystal [12]. In terms of the "Kato force" neutron current's behaviour in deformed crystal is determined by the equation

$$\frac{\partial^2 x}{\partial y^2} = \pm \frac{c}{m_0} f_k(y, x), \tag{15}$$

where $c \equiv \tan\theta_{\rm B}$ and $m_0 \equiv 2F_{\rm g}d/V$ is the so called "Kato mass" with $F_{\rm g}$ – the neutron structure amplitude and V – the unit cell volume. The sign $\pm$ in equation (15) corresponds to different Bloch waves.

In (15) the "Kato force" depends on the spatial coordinates X and Y (see Fig. 1). It can be easily demonstrated that putting an undeformed perfect crystal in a force field affecting the neutron along the reciprocal lattice vector g, we will have the same result as for a deformed crystal. So, the theory which was developed for weakly deformed crystals also works well in the presence of any external field affecting the diffracting neutron in undeformed crystal. An external field affecting a diffracting neutron was considered in [13].

It is also easy to show that an external force $\mathbf{F}_{\rm n}$ acting on a neutron along vector $\mathbf{g}$ (X axis, see Fig. 1) is equivalent to a gradient of interplanar distance with the value

$$\xi_{\rm f} = \frac{F_{\rm n}}{2E_{\rm n}}, \tag{16}$$

where $E_{\rm n}$ is the neutron energy.

Therefore the neutron trajectory equation (15) in the crystal in the presence of an external field will have the form

$$\frac{\partial^2 z}{\partial y^2} = \pm \frac{c^2 g}{2m_0} \frac{F_{\rm n}}{2E_{\rm n}}. \tag{17}$$

Let's compare this equation for the "Kato trajectory" with that for a usual trajectory of a neutron under the same external field in free space. The last one is described by standard Newtonian equation which has the form

$$\frac{\partial^2 z}{\partial y^2} = \frac{F_{\rm n}}{2E_{\rm n}}. \tag{18}$$

As it follows from (17) and (18) the "curvature" of the diffracting neutron trajectory in the crystal is magnified by the factor

$$K_{\rm e} = \pm \frac{c^2 g}{2m_0}. \tag{19}$$

This factor depends on the Bragg angle as $c^2 \equiv \tan^2 \theta_{\rm B}$, so for Bragg angles $\theta_{\rm B} \approx (84 - 88)^0$ influence of deformation can be intensified by a factor $\sim 100 - 1000$ as compared with a Bragg angle of $\sim 45^0$.

The numerical calculation of the factor $K_{\rm e}$ for (220) silicon crystallographic planes gives

$$K_e^{(220)} = \pm 0.85 \cdot 10^8, \tag{20}$$

for a Bragg angle $\theta_{\rm B} = 87^0$ (c=20).

Therefore, a 10 cm long crystal is equivalent to $\sim$ 1 km of free flight. The diffraction enhancement of the angular deflection of a neutron trajectory inside a crystal is well known, see for instance [14], but we have to note that such an effect can be considerably magnified by an additional gain factor proportional to $\tan^2 \theta_{\rm B}$ for Bragg angles close to $\pi/2$ [15]. The observed effects give us a chance to build a device with unprecedented sensitivity to external force acting on a neutron.

5. Possible application of two-crystal diffraction scheme. m_i/m_G experiment with neutron

Principle scheme of the setup is based on two-crystal scheme of diffraction as it was shown in Fig. 2. The necessary high collimation of the beam was provided by the first crystal with slits placed on entrance and exit surfaces, for details see [14]. An external force which is parallel to the reciprocal lattice vector curves the neutron trajectories inside the crystals. This results in a shift of the neutron beam along the exit surface of the second crystal:

$$\Delta_F^1(1,2) = \pm \frac{\pi\, c^2 L^2}{m_0 d\, E_{\rm n}} F_{\rm n} \equiv \pm \Delta_F^1, \tag{21}$$

where $\pm$ corresponds to the two type of Bloch waves excited in a crystal.

After averaging over "Pendellosung" oscillations which arise due to the interference of $\psi(1)$ and $\psi(2)$ and in case of large crystal (see section 2) we get the shift of the neutron beam along the second crystal exit surface

$$\Delta_{\rm S} = \Delta_F^1 = \frac{\pi\ c^2 L^2}{m_0 d\ E_{\rm n}} F_{\rm n}. \tag{22}$$

The resolution of the external force, i.e. magnitude of force when the neutron beam shift $\Delta_{\rm S}$ is equal to the slit size δ_s, is equal to:

$$F_{\rm W} = \frac{m_0 d\ E_{\rm n}}{\pi\ c^2 L^2} \delta_s \tag{23}$$

One of the applications can be connected with the measurement of inertial to gravitational neutron mass ratio. Our Earth is moving at a stationary orbit around the Sun, it means that the gravitational force which is proportional to the gravitational mass is in balance with the centrifugal force which is proportional to the inertial mass. If this is not so for free neutrons, then in the coordinate system connected with the Earth a free neutron will feel a non zero force[1]

$$F_{\rm m} = \frac{(m_i - m_G) \cdot G M_S}{R_S^2} \approx \Delta_{Gi} \cdot 6 \cdot 10^{-4} m_G g \tag{24}$$

where m_G and m_i are the neutron gravitational and inertial masses, G is the gravitational constant, M_S is the mass of the Sun, R_S is the distance to the Sun, $\Delta_{\rm Gi} \equiv (m_i - m_G)/m_G$. Moreover, this force will oscillate in the laboratory coordinate system with one day period due to the Earth spinning motion, see Fig. 5.

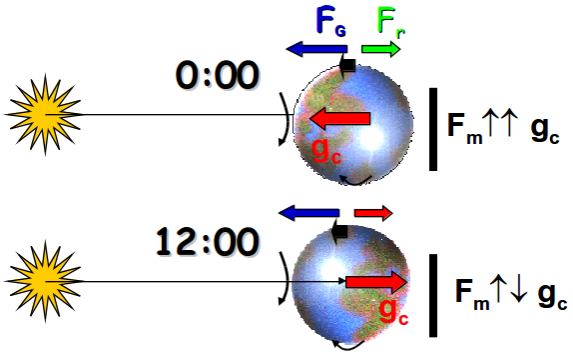

Figure 5: Position of the setup relatively to the Sun. $\mathbf{g}_c$ is the setup orientation.

Conclusions

The good agreement of experimental results with theoretical predictions based on specific dynamical diffraction speculations was shown. With taking Borrmann effect into account absorption

[1]The idea of this experiment is an analogue to the well known Eõtvõs experiment for the equivalence principle checking [16]

length for low-absorbed Bloch wave for (220) silicon plane is by one order of magnitude higher compared to non-diffracted neutron.

Observed dynamical diffraction effects discussed in this paper give a chance to measure any small external force acting on a neutron with unprecedented sensitivity. Preliminary estimations and test experiments [1, 17] showed us that the possible sensitivity to external force can reach the magnitude

$$\sigma(F_{ext}) \cong 10^{-17} \text{ eV/cm},$$

which provides us for instance measuring m_i/m_G ratio with the accuracy $\sigma(m_i/m_G) \sim 10^{-5}$ for the available silicon crystal and cold neutron beam flux. This is more than one order of magnitude better than the best modern result [18].

This work was supported by RFBR (grants 11-02-00188 and 11-02-12161-ofi-m-2011) and program of Russian Ministry of Sciense and Education (grant 2.1.1/12359).

References

[1] *V.V. Voronin, I.A. Kuznetsov, E.G. Lapin, S.Yu. Semenikhin, V.V. Fedorov*, Physics of Atomic Nuclei, 72, 3, 470 (2009)

[2] *V.V. Voronin, V.V. Fedorov, I.A. Kuznetsov , E.G. Lapin, S.Yu. Semenikhin, Yu.P. Braginetz, E.O. Vezhlev*, Physics Procedia, 17, 2011, P. 232–238.

[3] *V.V. Voronin, I.A. Kuznetsov, E.G. Lapin, V.V. Fedorov*, JETP Lett., 71, 76 (2000).

[4] *A. Zeilinger, C.G. Shull, M.A. Horne and K.G. Finkelstein*, Phys. Rev. Lett., 57, 3089 (1986).

[5] *G. Borrmann*, Z.Physik, 42, 157 (1941).

[6] *H. Rauch and D. Petrachek*, In Neutron diffraction/ ed. by H. Duchs, Berlin:Springer, 1978, P. 303-351.

[7] *Yu. Kagan, A.M. Afanasiev*, JETP, 49, 1504 (1965).

[8] *Yu. Kagan, A.M. Afanasiev*, JETP, 59, 271 (1966).

[9] *J.W. Knowles*, Acta Cryst. 9, 61 (1956).

[10] *N. Kato*, Acta Cryst. 13, 349 (1960).

[11] *V.I. Indenbom, I.Sh. Slobodetsky, K.G. Truni*, JETP, 66, 1110 (1974).

[12] V.L. Alexeev, E.G. Lapin, E.K. Leushkin, V.L. Rumiantsev, O.I. Sumbaev, V.V. Fedorov, JETP **94**, 371 (1988)

[13] S.A. Werner, Phys. Rev. B **21**, 1774 (1980)

[14] A. Zeilinger, C.G. Shull, M.A. Horne, K.G. Finkelstein, Phys. Rev. Lett. **57**, 3089 (1986)

[15] V.V. Fedorov, I.A. Kuznetsov, E.G. Lapin, S.Yu. Semenikhin, V.V. Voronin, JETP Lett. **85**, 82 (2007)

[16] R.V. Eotvos, D. Pekar, and E. Fekete, Ann. Phys. (Leipzig) **68**, 11 (1922)

[17] *V. V. Voronin, Yu. P. Braginetz, E. O. Vezhlev, I. A. Kuznetsov, E. G. Lapin, S. Yu. Semenikhin, V. V. Fedorov*, PNPI Preprint-2849. Gatchina, 2010.

[18] *J. Schmiedmayer*, Nucl. Instr. Meth. A 284, 59 (1989)